

# PROCEEDINGS OF SPIE

[SPIDigitalLibrary.org/conference-proceedings-of-spie](https://spiedigitallibrary.org/conference-proceedings-of-spie)

## MTF and PSF measurements of the CCD273-84 detector for the Euclid visible channel

I. Swindells, R. Wheeler, S. Darby, S. Bowring, D. Burt, et al.

I. Swindells, R. Wheeler, S. Darby, S. Bowring, D. Burt, R. Bell, L. Duvet, D. Walton, R. Cole, "MTF and PSF measurements of the CCD273-84 detector for the Euclid visible channel," Proc. SPIE 9143, Space Telescopes and Instrumentation 2014: Optical, Infrared, and Millimeter Wave, 91432V (28 August 2014); doi: 10.1117/12.2053005

**SPIE.**

Event: SPIE Astronomical Telescopes + Instrumentation, 2014, Montréal, Quebec, Canada

# MTF and PSF measurements of the CCD273-84 detector for the Euclid visible channel

I. Swindells\*<sup>a</sup>, R. Wheeler<sup>a</sup>, S. Darby<sup>a</sup>, S. Bowring<sup>a</sup>, D. Burt<sup>a</sup>, R. Bell<sup>a</sup>,  
L. Duvet<sup>b</sup>, D. Walton<sup>c</sup>, R. Cole<sup>c</sup>

<sup>a</sup>e2v technologies (UK) Ltd, 106 Waterhouse Lane, Chelmsford, CM1 2QU, UK

<sup>b</sup>European Space Agency, Keplerlaan 1, 2200AG Noordwijk, The Netherlands

<sup>c</sup>Mullard Space Science Laboratory, Holmbury St. Mary, Dorking, Surrey RH5 6NT, UK

## ABSTRACT

The European Space Agency (ESA) and e2v, together with the Euclid Imaging Consortium, have designed and manufactured pre-development models of a novel imaging detector for the visible channel of the Euclid space telescope. The new detector is an e2v back-illuminated, 4k x 4k, 12 micron square pixel CCD designated CCD273-84. The back-illuminated detectors have been characterised for many critical performance parameters such as read noise, charge transfer efficiency, quantum efficiency, Modulation Transfer Function and Point Spread Function. Initial analysis of the MTF and PSF performance of the detectors has been performed by e2v and at MSSL and the results have enabled the Euclid VIS CCD project to move in to the C/D or flight phase delivery contract. This paper describes the CCD273-84 detector, the test method used for MTF measurements at e2v and the test method used for PSF measurements at MSSL. Results are presented for MTF measurements at e2v over all pre development devices. Also presented is a cross comparison of the data from the MTF and PSF measurement techniques on the same device. Good agreement between the measured PSF Full Width Half Maximum and the equivalent Full Width Half Maximum derived from the MTF images and test results is shown, with results that indicate diffusion FWHM values at or below 10 micron for the CCD273-84 detectors over the spectral range measured. At longer wavelengths the diffusion FWHM is shown to be in the 6-8 micron range.

**Keywords:** Euclid, CCD, PSF, MTF.

## 1. INTRODUCTION

The ESA Euclid medium class mission will be launched at the end of the decade and aims to understand the role of dark matter and energy in the evolution of the universe. The visible channel used to measure the shapes of billions of galaxies will be made up of 36 e2v CCD273-84 detectors. The CCD273-84 detector is nominally a 4k x 4k back-illuminated CCD, consisting of two 2066 x 4096 image sections of 12  $\mu\text{m}$  square pixels separated by a parallel charge injection structure. There are 2 readout registers which can operate in a split transfer mode for signal read out through the 4 high-responsivity, low noise output circuits<sup>1</sup>.

Characterisation of the performance of the CCD273-84 is a critical activity for the Euclid Imaging Consortium. Development of CCD test benches at ESA<sup>2</sup> as well as at Mullard Space Science Laboratory (MSSL) aim to provide facilities to this end. Critical to the detectors ability to determine faint galaxy shapes is the Point Spread Function (PSF) characteristic. PSF performance has been measured at MSSL on CCD273-84 detectors as part of the Euclid pre-development phase and some of those results along with the test setup and method are presented in this paper. Initial CCD testing however is performed at e2v during detector assembly and screening. A dedicated test bench has been commissioned to measure detector parameters such as readout noise, quantum efficiency and charge transfer efficiency. As was developed for the Gaia CCD detectors, a separate test system has also been commissioned at e2v to measure Modulation Transfer Function (MTF) for device screening purposes in place of PSF measurements. This is to ease the test complexity and enable production testing to be performed in a time as to meet the mission launch date. Details of the MTF test system and measurement method are described. Results of MTF testing on 11 back-illuminated CCD273-84 devices as part of the Euclid pre-development phase are presented along with a comparison between the MTF and PSF results measured on the same detector at e2v and at MSSL.

## 2. MTF MEASUREMENT TECHNIQUE AT E2V

Modulation Transfer Function is defined theoretically in terms of the response to a sinusoidally modulated “parallel bar pattern” input. However, the pixelated nature of CCDs makes it difficult to measure MTF in these terms and this input pattern has not been used at e2v. Instead an operational or ‘pseudo’ MTF can be calculated by analysing the line response function (LRF) for a single pixel. The line response function is defined as the relative response to an infinitesimally narrow line imaged on the pixel at a various distances from the centre of the pixel. A method known as the Vernier Technique is used at e2v to measure the line response function, in which the displacement of the line is achieved by tilting the line slightly and sampling over successive pixel rows. This test method has been used as the standard method at e2v for many years and is used here to provide consistency of results. The experimental setup for the MTF measurements is shown in figure 1. The CCD is mounted on a three axis movement stage arrangement to allow accurate positioning in X and Y and for fine focusing in the Z axis. Colour LEDs and optical narrowband filters (bandwidth 10 nm) are used to measure MTF between 500 nm and 900 nm. The 10 µm slit is de-magnified by a factor of 20 so at the focus point it would be 0.5 µm wide. Due to the practical difficulties in focusing the slit through a window, the device is not under vacuum but is in an enclosed chamber purged with Nitrogen to allow moderate cooling to 5 °C to reduce background dark signal. Horizontal (X) and vertical (Y) MTF is measured in one location of the amplifier G image section. The location selected is a worst-case for charge transfer inefficiency (CTI) contribution, as it requires the maximum number of transfers to read out the data and therefore incorporates the maximum CTI. There is no CTI subtraction performed during analysis.

The narrow slit image is focused onto the CCD angled with a gradient of approximately 1 pixel horizontally for each 8 vertical pixels for horizontal MTF (the slit is rotated by 90° for vertical MTF measurements). The focusing routine involves an automated iteration of the Z axis position to minimize the measured line width. Ten dark images are averaged and subtracted pixel by pixel from the average of ten illuminated slit images to produce the 16x16 pixel image of the slit (see figure 2). The position and gradient of the image of the slit is determined from the pixel signal values in each row. An LRF function is then constructed using the pixel signal value and distance from the slit. The measured LRF points are then interpolated to get a regularly sampled LRF. This LRF is then Fourier Transformed to produce a plot of MTF versus sampling frequency (see figure 3). The MTF is normalised to 1 at zero frequency and multiplied by 100 to covert to %. Sampling frequency is in fractions of the Nyquist Frequency, defined in terms of pixel pitch  $p$  (in mm) as

$$F_{Ny} = 1/2p . \quad (1)$$

The MTF calculated in this way is the Total measured MTF, which is assumed to be the product of the Diffusion, Geometrical and Optical MTF contributions:

$$MTF_T = MTF_D \times MTF_G \times MTF_O. \quad (2)$$

The optical MTF is due to the microscope objective used to focus the slit. The optical MTF at each wavelength has been measured for this type of microscope objective and this is corrected for in the MTF analysis to yield the MTF at Nyquist values ( $MTF_{Ny} = MTF_T/MTF_O$ ) reported and used by e2v to assess device performance and acceptance criteria.

## 3. E2V MTF RESULTS ON CCD273-84 DEVICES

Back-thinned CCD273-84 devices were produced and tested at e2v as part of the ESA pre-development phase for the VIS CCD detectors. Devices came from 2 silicon fabrication batches and 11 were tested for MTF, 8 from silicon batch 11312 and 3 from silicon batch 11263. The MTF at Nyquist results averaged for all 11 devices are summarised in table 1. The peak pixel signal level is approximately 50% of pixel saturation with 3 image phases held high during integration.

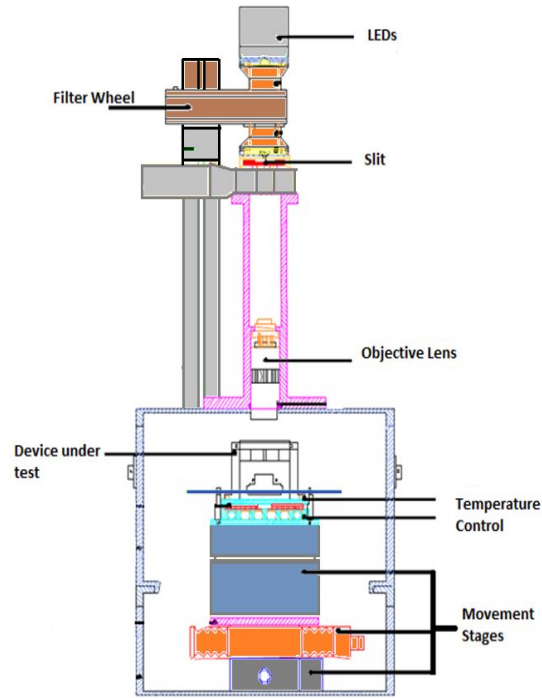


Figure 1. MTF measurement setup. See text for detailed description.

As expected for a back-thinned CCD, the MTF improves at longer wavelengths. This is related to increased absorption depth in silicon for longer wavelength light and the decrease in the fraction of photoelectrons generated in the un-depleted region and spreading laterally before collection. With an increasing un-depleted region at the back surface, the MTF at blue wavelengths falls significantly compared to that at red wavelengths. The depletion depth,  $x_d$ , can be calculated under each electrode for the CCD273-84 pixel using

$$x_d = \sqrt{\frac{2\epsilon_{Si}}{qN_A} (\phi_c - V_{ss})} + x_c \quad (3)$$

where  $\epsilon_{Si}$  is the permittivity of silicon ( $1.04 \times 10^{-12}$  F/cm),  $q$  is the electron charge ( $1.6 \times 10^{-19}$  C),  $N_A$  is the doping concentration per  $\text{cm}^3$ ,  $(\phi_c - V_{ss})$  is the potential across the channel to substrate and  $x_c$  is the buried channel depth which is taken as fully depleted. Using the parameters listed in table 2, and assuming 3 phases high storing charge and 1 phase low per pixel and  $1.5 \mu\text{m}$  column isolation ‘dead region’ at both sides of the pixel, a pixel average depletion depth is calculated via equation (3) to be  $x_d = 36.2 \pm 1.9 \mu\text{m}$ .

Wavelength (nm)	Horizontal MTF at Nyquist (%)		Vertical MTF at Nyquist (%)	
	Mean	Std. Dev.	Mean	Std. Dev.
500	37.1	2.0	43.0	0.9
600	37.0	1.1	44.1	0.7
700	39.0	2.6	45.4	2.7
800	45.3	1.9	49.5	1.0
900	46.8	1.1	47.9	0.8

Table 1: Horizontal (X) and Vertical (Y) MTF at Nyquist results for all 11 CCD273-84 devices tested at e2v.

Parameter	Value
Buried channel depth $x_c$	$0.9 \pm 0.1 \mu\text{m}$
Doping concentration $N_A$	$1.0 \pm 0.1 \times 10^{13} \text{ cm}^{-3}$
Signal charge density	$10 \pm 1 \text{ ke}/\mu\text{m}^2$
Charge capacity	$1.50 \pm 0.25 \text{ ke}/\mu\text{m}^2/\text{V}$
Channel potential $\phi_{ch0}$	$10.3 \pm 0.2 \text{ V}$
Image clock High, Low	8, 0 V

Table 2: Input parameters to depletion depth calculation. Only the image clock voltages and channel potential are measured factors, the other parameters are estimated from expectations of typical values for general CCDs and for the signal level in the images.

An MTF model based on a solution of the classic continuity equation has been used for calculating the theoretical MTF values for the CCD273-84 pixel. Figure 4 shows the calculated geometric MTF based on the pixel pitch,  $12 \mu\text{m}$ , and photosensitive fraction, 100%. The diffusion MTF is determined via a fast Fourier transform of a derived line response function based on the device thickness,  $40 \mu\text{m}$ , the carrier diffusion length, assumed to be  $100 \mu\text{m}$ , the wavelength and depletion depth. The modeled MTF at Nyquist versus wavelength is shown in figure 5 for un-depleted depths of  $4 \mu\text{m}$  and  $6 \mu\text{m}$  plotted against the MTF results for CCD273-84 device 11312-14-01 (used later for PSF comparison). The measured data is generally in agreement with an un-depleted depth of  $4\text{--}6 \mu\text{m}$ , and in line with expectations based on MTF measurements made at e2v on other back-illuminated high resistivity CCDs (e.g. the Gaia RP devices). At  $500 \text{ nm}$  the results agree well with the modelled  $4 \mu\text{m}$  un-depleted depth whereas at  $800 \text{ nm}$  the results are closer to the modelled  $6 \mu\text{m}$  un-depleted depth. At  $900 \text{ nm}$  an even greater un-depleted depth is suggested but this variation is more likely due to other effects being present rather than real changes in depletion depth with wavelength.

The deviation of the data from the model trend with wavelength could be down to factors that affect measurement or due to assumptions made in the model. At long wavelengths, photons can pass through the pixel and reflect off the front side electrodes. If this reflection is at an angle then it is possible than photons entering the CCD in one pixel can actually create charge in a neighbouring pixel resulting in lower MTF. This multi-pass reflection effect is not included in the MTF model. Also, depth of focus effects may be significant for long wavelengths with high numerical aperture optics. The input to the model also uses the average depletion depth over the active width of the pixel as calculated above, where the active width is taken as the silicon between the columns isolation regions. However, for the CCD273-84 pixel there is  $1.5 \mu\text{m}$  column isolation at both sides of the pixel reducing the active pixel width to only  $9 \mu\text{m}$ . A more complete model for depletion in the pixel may be needed when the column isolation region is such a significant fraction of the pixel size as assuming it is a 'dead zone' for charge generation may not be completely accurate. The influence of the column isolation region may also explain why the measured horizontal MTF results are lower than the vertical MTF results, although there is no definitive model to explain this at the current time.

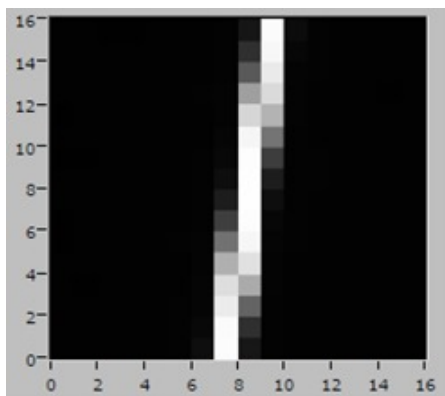


Figure 2. Image of the slit used for MTF measurement, resulting from subtracting pixel by pixel the average of 10 lit images from the average of 10 dark (un-illuminated) images.

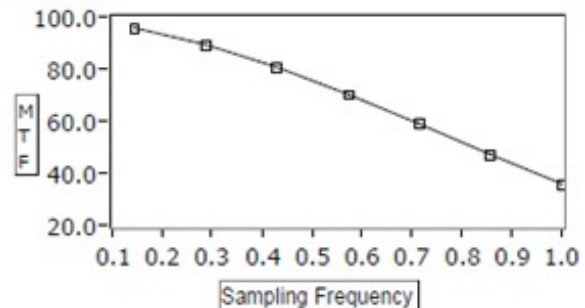


Figure 3. MTF (%) versus sampling frequency plot that results from the Fourier Transform of the measured line response function. Sampling frequency is in fractions of Nyquist Frequency and optical MTF has been factored out.

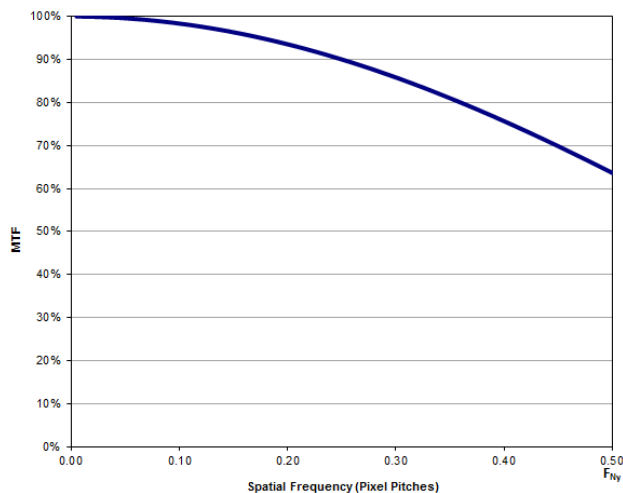


Figure 4. Geometrical MTF for CCD273-84 pixel, 12 mm pixel pitch 100% photosensitive fraction.

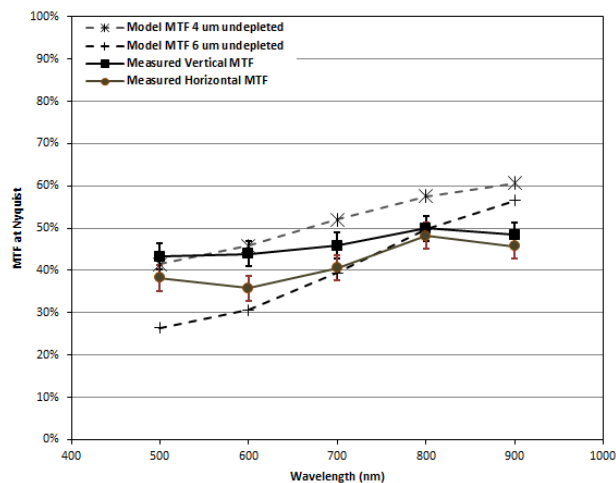


Figure 5. Measured vertical and horizontal MTF at Nyquist for device serial number 11312-14-01 against modelled MTF at Nyquist for 4  $\mu\text{m}$  and 6  $\mu\text{m}$  undepleted region. The error bars are 1-sigma uncertainty resulting from analysis during the Gaia project of the same method and test equipment used for the Euclid tests.

#### 4. PSF MEASUREMENT TECHNIQUE AND RESULTS AT MSSL

The experimental setup for PSF measurements is shown in figure 6. The CCD is mounted inside the vacuum chamber on a motorized X-Y stage for accurate positioning. A microscope objective lens is also mounted inside the chamber to focus and de-magnify the 10  $\mu\text{m}$  pinhole illumination. The light source and pinhole are on a Z-axis micrometer stage to allow focusing. The optical spot created by the light source in this way was demonstrated to be sufficiently sub-pixel, with a Gaussian FWHM of 1.5  $\mu\text{m}$ , by means of measuring the response of a photo-diode to a knife-edge moving across the focal plane in 0.5  $\mu\text{m}$  steps. The system is focused by recording an image and fitting two Gaussians (one in CCD X axis, the other in Y) to the image spot, and moving the Z-axis micrometer to minimise the spot width. PSF was measured using a focused spot for five different positions on the CCD (two in the E quadrant and one in each of F, G and H) at -90  $^{\circ}\text{C}$ . At each position, three wavelengths were used, 500, 700 and 900 nm. To compute the PSF from the images, a Gaussian fit to the pixel values around the peak of the spot is performed. The resulting characteristic width of the Gaussian is then multiplied by 2.355 to convert it to a FWHM. The measurement of the charge is quantised in the spatial domain due to the geometrical pixel pitch (P) of the charge collection regions. This adds quantisation noise of  $\pm P$ , which has a standard deviation of  $\frac{1}{\sqrt{12}}P$ , to the signal profiles used in the Gaussian fit. This is analogous to the  $\pm$  LSB quantisation noise with  $\frac{1}{\sqrt{12}}\text{LSB}$  standard deviation added when digitizing an analogue signal in electronics<sup>3</sup>. Therefore, to calculate the true PSF width in pixel pitches, a value of 0.289 ( $=\frac{1}{\sqrt{12}}$ ) is subtracted in quadrature from the width of the fitted Gaussian.

Using the method described above, the PSF was measured at MSSL on CCD273-84 device 11312-14-01. The results are shown in figure 7. A PSF FWHM of 7.8  $\mu\text{m}$  to 8.5  $\mu\text{m}$  is measured at 500 nm for horizontal (X) and vertical (Y) directions respectively. This falls to 7.0  $\mu\text{m}$  and 8.0  $\mu\text{m}$  at 900 nm for horizontal (X) and vertical (Y) directions. The signal level is around 50% to 75% of pixel saturation. The trend with wavelength is the inverse of the MTF results, which is as expected based on the relationship of higher MTF means lower PSF. The PSF values in the X direction are lower than in Y, which is contrary to the MTF results which would suggest the Y direction should have lower PSF. The reason for this discrepancy is not clear, it may be that using a slanted slit over many rows has a very different interaction

with the column isolation regions than using a point source for illumination in the centre of one pixel. More detailed modelling or measurements would be needed to fully understand this effect.

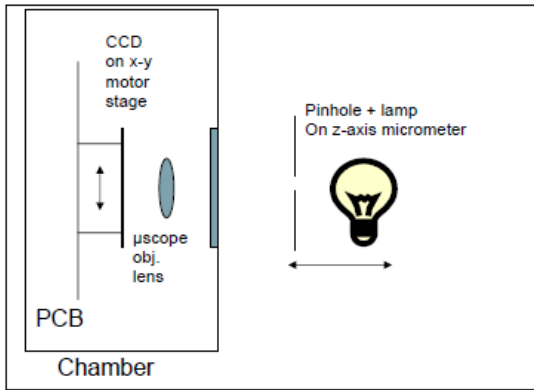


Figure 6. PSF measurement setup. See text for detailed description.

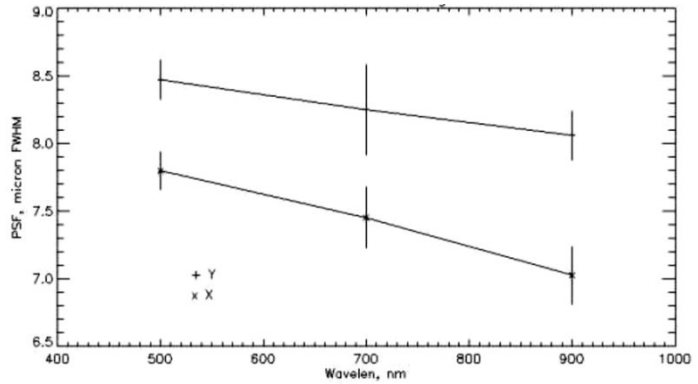


Figure 7. Mean PSF as a function of wavelength for CCD273-84 device 11312-14-01 averaged over 5 spot positions. The error bars represent the repeatability error variation over the 5 measurements.

## 5. COMPARISON OF PSF AND MTF RESULTS

The first method used to compare the results is to analyse the raw images used for MTF measurements and determine the FWHM of a Gaussian fit to the pixel signals along a row or column perpendicular to the line of the slit. The Gaussian fit was done on the row where the central pixel had the highest signal, which indicates the slit is closest to the centre of the pixel and therefore is a best match to the position of the spot for the MSSL measurements. This comparison is shown in figure 8. Although the PSF test at MSSL and the MTF test at e2v are set up to measure different parameters in different ways, analysis of the images produced in both tests show good agreement for FWHM values found by fitting Gaussian distributions to the pixel response.

A second method to compare the measurements is to determine the diffusion component of MTF and find the equivalent FWHM from a LRF model. Using equation (2) it is possible to remove the optical and geometric MTF from the total MTF measured results. With ideal measurement conditions, the remainder is then a measure of the diffusion MTF ( $MTF_D$ ):

$$MTF_D = MTF_T / (MTF_G \times MTF_o) \quad (4)$$

In reality there will be other contributions due to factors not accounted for, such as depth of focus, width of the slit image, front surface reflections etc so in this analysis these factors are included in the diffusion MTF. The measured MTF values and derived diffusion MTF using equation (4) are shown for device 11312-14-01 in tables 3 and 4. By making the assumption that the diffusion component has a Gaussian LRF, it can be modelled using:

$$LRF(x) = \frac{1}{\sqrt{2\pi}\sigma} \cdot \exp\left[\frac{-1}{2\sigma^2} \cdot (x - \mu)^2\right] \quad (5)$$

where;  $x$  is the distance in pixels (or microns),  $\mu$  is the mean of the distribution and  $\sigma$  is the standard deviation.

Performing a Fourier Transform on  $LRF(x)$  produces an MTF versus spatial frequency plot (figure 9). By varying the Gaussian FWHM ( $= \sigma \times 2.355$ ), a diffusion MTF at Nyquist versus FWHM plot can be made and a relationship between them derived (figure 10). Using this relationship, an equivalent Gaussian FWHM value can be calculated for the  $MTF_D$  results. These are also shown in tables 3 and 4. Comparing the calculated diffusion FWHM results and the measured MSSL values sees the same trend with wavelength and values in the same range, approximately 8-10  $\mu\text{m}$  at short wavelengths falling to 6-8  $\mu\text{m}$  at long wavelengths. As was seen in figure 8, the MTF derived FWHM vertical to

horizontal trend is reversed compared to that derived from the PSF measurements, but a full explanation for this is not known at the current time. The difference in test temperature between the acquired PSF images and MTF image is not accounted for in the analysis. MTF behaviour of CCDs can be shown to be temperature dependent in the mid-wavelength range due to changes of the silicon band gap voltage. The MTF model used in section 3 estimates that in the 700 nm range a decrease of 100 °C would produce ~ 4 % absolute increase in MTF at Nyquist, which is equivalent to ~ 0.5  $\mu\text{m}$  reduction in FWHM using figure 10. At the bluer and redder wavelengths, MTF change due to temperature is significantly less.

Performing the above analysis to all MTF measurements from all 11 devices represented in table 1 results in a maximum FWHM value of 10.1  $\mu\text{m}$  measured at the lower wavelength of the range. At the longer red wavelengths the values measured are in the 6-8 $\mu\text{m}$  range. This seems in line with the goals for the VIS detector as outlined in the ESA CCD requirements, given that these values are likely to be an over-estimation of the true FWHM from a point source.

Wavelength (nm)	MTF <sub>T</sub> (%)	MTF <sub>G</sub> (%)	MTF <sub>O</sub> (%)	Derived MTF <sub>D</sub> (%)	Equivalent FWHM ( $\mu\text{m}$ )
500	35.9	63.7	94.0	60.0	9.1
600	33.5	63.7	93.5	56.2	9.7
700	37.8	63.7	93.0	63.7	8.5
800	44.1	63.7	91.5	75.7	6.7
900	40.7	63.7	89.0	71.7	7.3

Table 3: Measured horizontal MTF for device 11312-14-01 and equivalent FWHM of the Gaussian LRF needed to produce the derived diffusion MTF.

Wavelength (nm)	MTF <sub>T</sub> (%)	MTF <sub>G</sub> (%)	MTF <sub>O</sub> (%)	Derived MTF <sub>D</sub> (%)	Equivalent FWHM ( $\mu\text{m}$ )
500	40.7	63.7	94.0	68.0	7.9
600	41.0	63.7	93.5	68.9	7.8
700	42.7	63.7	93.0	72.1	7.3
800	45.7	63.7	91.5	78.3	6.3
900	43.1	63.7	89.0	76.0	6.7

Table 4: Measure vertical MTF for device 11312-14-01 and equivalent FWHM of the Gaussian LRF needed to produce the derived diffusion MTF.

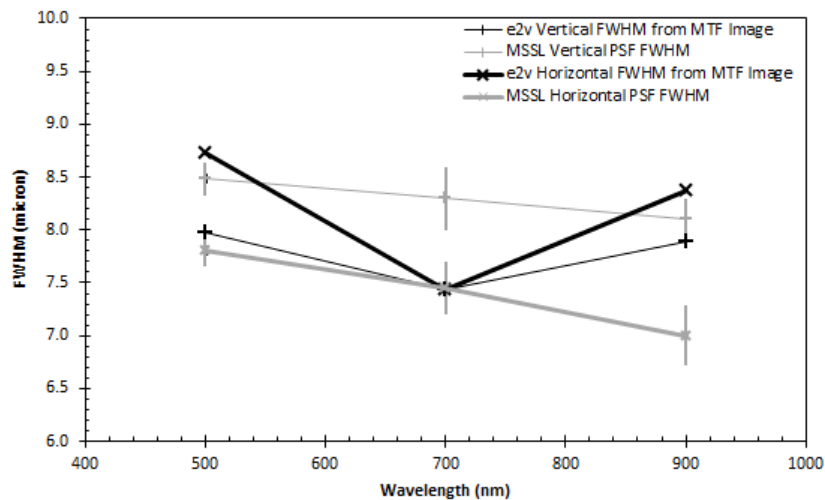


Figure 8. Device 11312-14-01 vertical and horizontal MSSL PSF and e2v MTF Image Gaussian fit FWHM results. The pixilation (or quantization) effect has been subtracted out in both cases. As the e2 images were taken only once, no repeatability error can be included.

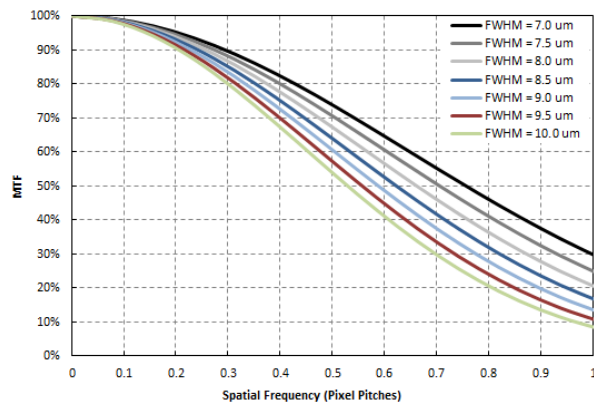


Figure 9. Diffusion MTF versus spatial frequency resulting from a Fourier transform of a Gaussian LRF with varying FWHM values.

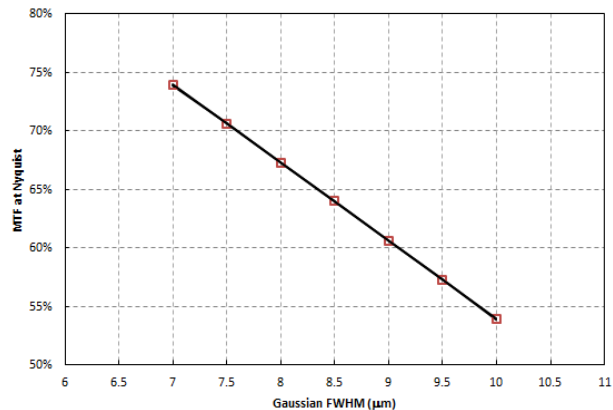


Figure 10. Resulting Diffusion MTF at Nyquist (0.5 pixel pitches) versus LRF Gaussian FWHM.

## 6. CONCLUSIONS

Back-illuminated CCD273-84 detectors have been designed and manufactured by ESA and e2v, together with the Euclid Imaging Consortium, as part of the pre-development phase of the Euclid VIS detector project. At e2v, 11 of these CCD273-84 devices were tested for MTF performance. The results are inline with previous measurements of MTF on back-illuminated high-resistivity CCDs such as the RP Gaia CCDs, although the results are somewhat lower than the MTF model predicts at red wavelengths. The model used is relatively basic and predicts only first order MTF values and doesn't take things such as front-surface reflections at long wavelengths in to account. From these 11 CCDs, one was also tested for PSF at MSSL. Analysis of the MTF images gives good agreement with the PSF FWHM values measured, as do values derived from the MTF results using a basic model for diffusion MTF. There is some contradiction between MTF and PSF as to whether the horizontal (X) or vertical (Y) performance is better, however all measurements and analysis from the PSF and MTF results indicate diffusion FWHM values at or below 10  $\mu\text{m}$  for the detectors over the full wavelength range measured. At longer wavelengths the FWHM values are in the 6-8  $\mu\text{m}$  range.

## 7. REFERENCES

- [1] Endicott, J., "Charge-Coupled Devices for the ESA Euclid M-class Mission," Proc. SPIE 8453, 845304-1 (2012).
- [2] Verhoeve, P., "ESA's CCD test bench for the Euclid visible channel," Proc. SPIE 8453, 845322 (2012).
- [3] Smith, S., "The Scientist and Engineer's Guide to Digital Signal Processing," California Technical Publishing, 3, 35 (1997). <http://www.dspguide.com/ch3/1.htm>.